JOURNAL OF CATALYSIS 107, 181–194 (1987)

$AlPO_4$-Supported Nickel Catalysts

VIII. Support Effects on the Gas-Phase Dehydrogenation of Alkylbenzenes

F. M. BAUTISTA, J. M. CAMPELO,[1] A. GARCIA, D. LUNA, AND J. M. MARINAS

Department of Organic Chemistry, Sciences Faculty, Cordoba University, E-14004 Cordoba, Spain

Received November 20, 1986; revised February 18, 1987

The nonoxidative dehydrogenation of alkylbenzenes (ethylbenzene, *n*-propylbenzene, and isopropylbenzene) has been carried out at 625–850 K on nickel catalysts at 20 wt% supported on Al_2O_3, SiO_2, and two different types of $AlPO_4$. Furthermore, unsupported bulk nickel was employed as the catalyst. The acidic and basic properties and the surface area of the supports and supported nickel catalysts were measured as well. Unlike what is described for TiO_2–ZrO_2 catalysts, our observation was that the acid and basic sites do not exhibit catalytic activity in the nonoxidative dehydrogenation of alkylbenzenes. However, it appears that the acid–basic nature of the supports, through the effects of metal–support interaction, plays an important part in determining the specific catalytic activity of the supported nickel catalysts. These metal–support interaction effects, as well as the substituent effects, can be evaluated through several isokinetic parameters obtained from the existence of a linear correlation between the $\Delta H^{\neq}$ and $\Delta S^{\neq}$ activation parameters obtained from the Eyring equation (and between ln A and E_a, from the Arrhenius equation) known as the compensation effect. This is ascribed to the existence of a linear free-energy relationship (LFER) in a set of gas-phase reactions similar to that previously described for the liquid-phase hydrogenation of allyl alcohols on the same nickel-supported catalysts.

INTRODUCTION

In heterogeneous catalytic processes the influence of the substrate structure as well as the influence of catalysts on reactivity are topics of special interest. In a previous paper (*1*), the existence of a "isokinetic relationship" or "compensation effect" was obtained in the liquid-phase catalytic hydrogenation of allyl alcohols over a series of supported nickel catalysts. This compensation effect was associated with the existence of a linear free-energy relationship (LFER) and there seems to be a general pattern of behavior in the liquid-phase catalytic hydrogenation process that could provide a means of classification not only for reaction series and mechanisms but also for catalyst series.

Although recently the compensation effect has been designated as a specific feature of liquid-phase reactions (*2*), there has long been a feeling among kineticists that solvent effects are basically more complicated and more specific than substituent effects (*3, 4*). For this reason we think that there is a current interest in the study of the application of LFER in the field of heterogeneously catalyzed gas-phase reactions, whose quantitative study is now becoming possible due to advances in technology.

With respect to this, the present paper reports the results of an ongoing study on the nonoxidative dehydrogenation of some alkylbenzenes (R = Et, *n*-Pr, and i-Pr) over a series of nickel catalysts at 20 wt% supported on Al_2O_3, SiO_2, and two different types of $AlPO_4$ synthesized according to Kearby (*5*), employing two different precipitation agents, ammonia and propylene oxide, $AlPO_4$-F and $AlPO_4$-P, respectively. These supported nickel systems were the

[1] To whom all correspondence should be addressed.

0021-9517/87 $3.00

same ones previously employed as catalysts in the individual and competitive liquid-phase hydrogenation of allyl alcohols (*1*) showing not only the importance of the role of the support in determining the adsorption and catalytic behavior of supported nickel systems but also the excellent behavior of aluminum phosphates as nickel supports. Furthermore, the existence of metal–support interactions was confirmed in $AlPO_4$-supported nickel catalysts previously described (*6–15*).

On the other hand, $AlPO_4$ is structurally similar to silica (*16, 17*) and exhibits surface acid and basic sites capable of catalyzing a number of reactions (*18–26*). Since the cooperative effect of the acid–base properties of the TiO_2–ZrO_2 catalyst has also been shown (*27–30*), further research on this reaction may be of interest to compare the results obtained with the supported nickel catalysts and those obtained using as the catalyst each support Al_2O_3, SiO_2, $AlPO_4$-F, and $AlPO_4$-P, or unsupported nickel.

EXPERIMENTAL

Catalysts

Four systems of nickel supported at 20 wt% were used as catalysts on the following supports: a commercial silica (SiO_2, Merck kieselgel 60, 70–230 mesh), a commercial alumina (Al_2O_3, Merck acidic for chromatography), and two aluminum orthophosphates prepared by precipitation from $Cl_3Al \times 6H_2O$ and H_3PO_4 (85 wt%) with aqueous ammonia ($AlPO_4$-F) or propylene oxide ($AlPO_4$-P). The resulting powders screened to <0.149 mm were calcined in air at 920 K for 3 h. Both commercial supports, Al_2O_3 and SiO_2, were subjected to the same calcination treatment.

The detailed synthesis procedure and textural properties of supports (surface area, pore volume, and main pore diameter) determined by nitrogen adsorption have been published elsewhere (*1, 23, 24, 26*) and are summarized in Table 1, where the surface basicity and acidity of supports are also collected. These values were determined by a spectrophotometric method, described elsewhere (*19, 23, 24*), that allows titration of the amount of irreversibly adsorbed benzoic acid ($pK_a = 4.19$) or pyridine ($pK_a = 5.25$) employed as titrant agents of basic and acid sites, respectively. The monolayer coverage at equilibrium at 298 K, X_m, is accomplished by applying the Langmuir adsorption isotherm, and it is assumed as a measure of the acid or basic

TABLE 1

Textural and Acid–Base Properties of the Different Supports

Support	S_{BET}[a] ($m^2\ g^{-1}$)	S_t[b] ($m^2\ g^{-1}$)	V[c] ($ml\ g^{-1}$)	d[d] (nm)	Acidity[e] ($\mu mol\ g^{-1}$)	Basicity[f] ($\mu mol\ g^{-1}$)
$AlPO_4$-F	156	152	0.68	2–4	190	200
$AlPO_4$-P	228	236	0.94	2–4	227	166
SiO_2	366	372	0.68	2–5	206	164
Al_2O_3	72	75	0.24	2–7	23	191

[a] Surface area, determined from BET method.
[b] Surface area from V–n plots.
[c] Pore volume.
[d] Main pore diameter.
[e] Monolayer coverage X_m at equilibrium at 298 K obtained with pyridine ($pK_a = 5.25$).
[f] Monolayer coverage X_m at equilibrium at 298 K obtained with benzoic acid ($pK_a = 4.19$).

sites corresponding to the specific pK_a of the base or acid used as the titrant.

Catalysts containing 20 wt% nickel were prepared by impregnation of the supports to incipient wetness with 10 M aqueous solutions of nickel nitrate. They were dried, crushed, and screened to a particle size <0.149 mm (100 mesh size), reduced in an ultrapure hydrogen stream (1.7 $cm^3\ s^{-1}$) at 673 K for 3 h, and then cooled to room temperature in the same hydrogen stream and stored in sealed glass bottles until required. A more detailed description of the synthesis procedure has been reported previously (*6, 9*). Bulk nickel was obtained by reduction of nickel oxide (Merck, p. a.) under the same conditions employed with the supported nickel systems.

Metal surface areas, S, of different catalysts have been previously obtained (*1*). They were determined from the average crystallite diameter, D, obtained by X-ray diffraction (XRD), according to the method of Moss (*31*) as has been described elsewhere (*1, 6–9, 13, 32*). X-ray line-broadening experiments were conducted with a Philips Model 1103/00/60 diffractometer, using Co$K\alpha$ radiation. A scan speed of 7.5° h^{-1} was used for the 2θ range between 46° and 56° because the width of the (111) nickel peak at half-height was used in line-broadening calculations. All XRD runs were carried out on powder samples of catalyst.

The metal surface area of bulk Ni has also previously been obtained (*13*) using XRD and transmission electron microscopy (TEM). The values obtained by both techniques were in very close agreement: S_{XRD} = 13.1 $m^2\ g_{Ni}^{-1}$ and S_{TEM} = 15.0 $m^2\ g_{Ni}^{-1}$, respectively.

Textural and acid–base properties of supported nickel catalysts have also been obtained in a similar way to that used with the supports. In fact, the spectrophotometric method employed lets us determine not only the surface acidity and basicity of white solids used as the supports, but also of deeply colored or black ones such as the nickel-supported catalysts. Table 2 summarizes the acid–base properties, the surface area, and the metal surface area of supported nickel catalysts.

TABLE 2

Acid–Base Properties, Surface Area, S_{BET}, Metal Surface Area, S, and Average Crystallite Diameter, D, of Supported 20 wt% Nickel Catalysts

Catalysts	D (nm)	S ($m^2\ g_{Ni^{-1}}$)	S_{BET} ($m^2\ g_{cat}^{-1}$)	Acidity[a] (μmol g^{-1})	Basicity[b] (μmol g^{-1})
Ni/$AlPO_4$-F	11.9	55.6	78	40	159
Ni/$AlPO_4$-P	20.9	32.2	65	42	142
Ni/SiO_2	15.1	44.5	264	106	82
Ni/Al_2O_3	25.2	26.8	60	15	178
Ni-bulk	59.7	13.1	[c]	[c]	[c]

[a] Pyridine, pK_a = 5.25.
[b] Benzoic acid, pK_a = 4.19.
[c] Negligible.

Apparatus, Materials, and Procedure

Dehydrogenation reactions were carried out in a conventional fixed-bed type reactor with a continuous-flow system at atmospheric pressure. The reactor was made of stainless steel tubing (15 mm in internal diameter and 120 mm long) placed in a tubular electric furnace and the prescribed temperature (625–850 K) was monitored by a thermocouple located in the reactor wall. Isothermal temperatures were measured within an accuracy of ±1 K. To obtain isothermal conditions, a known amount of catalyst (W = 0.1 g, <0.149 mm) was diluted with glass beads and placed between two layers of glass beads separated by glass wool until the reactor was packed from top to bottom. Fresh catalyst was used in each experiment.

The standard pretreatment of the catalyst consisted of heating in a stream of nitrogen (99.999%, H_2O < 3 ppm) of 2 $cm^3\ s^{-1}$ for 1 h at the reaction temperature.

In order to obtain different residence time (W/F = 70–7 × 10^3 g s mol^{-1}), W/F defined as the ratio of the weight of the catalyst, W (g), to the feed rate, F (mol s^{-1}), at a fixed catalyst weight of 0.1 g each substrate was fed at several rates (F in the

interval 10–0.1 cm^3 min^{-1}) by means of a microfeeder (Perfusor VI B. Braun).

The starting materials: ethyl- (EB), *n*-propyl- (*n*-PB), and isopropylbenzene (i-PB) were supplied by Merck p. a. and purified by distillation under reduced pressure and low temperature and then passed through active acidic aluminium oxide powder for chromatography (Merck) activated at 673 K in flowing ultrapure nitrogen.

The liquid products were collected by traps cooled with ice and dry ice, and analyzed on a 5720A Hewlett-Packard conventional gas-chromatograph with a 2 m × 0.3 mm (i.d.) stainless steel column packed with 5% polyphenylether on Chromosorb G-AW DMCS 80/100. The nitrogen carrier gas had a flowrate of 20 cm^3 min^{-1}. The temperature of the column was 373 K and that of the detector and injector was 473 K. Besides, a spectrophotometric analysis of the different samples was made due to the low conversion values obtained (<0.5%) at the higher F values. These experiments are developed at the wavelength of the maximum absorption of the dehydrogenation products in cyclohexane solutions (spectroscopic grade, Merck) and between the concentrations where the Lambert–Beer law fits (0.5 cm^3 of reaction product is diluted in 4.5 cm^3 of cyclohexane).

The gas chromatographic analysis for all runs indicated that the only reaction products obtained were those corresponding to the dehydrogenation reaction of the alkylbenzenes: styrene, α-, and β-methylstyrene, respectively.

RESULTS

The average particle size of the catalysts used (<0.149 mm) determines that the reactions were not influenced by internal diffusion. In order to select the range of working conditions where no external diffusional limitations exist, the dehydrogenation rates, R, (obtained for 0.1 g of catalyst at several feed rates, F) were represented against feed rate (F). The results obtained for the $Ni/AlPO_4$-F catalysts at 723 K with the three substrates are shown in Fig. 1a.

According to these results, the absence of external diffusion effects in the present experimental conditions are obtained for feed rates, F, over 1.2×10^{-4} mol s^{-1}. Thus, the bulk of the kinetic runs were performed at a fixed ratio of catalyst mass (0.1 g) and at least at three feed rates in the interval $1.2–14 \times 10^{-4}$ mol s^{-1}, at temperatures between 625–850 K. Thus, the con-

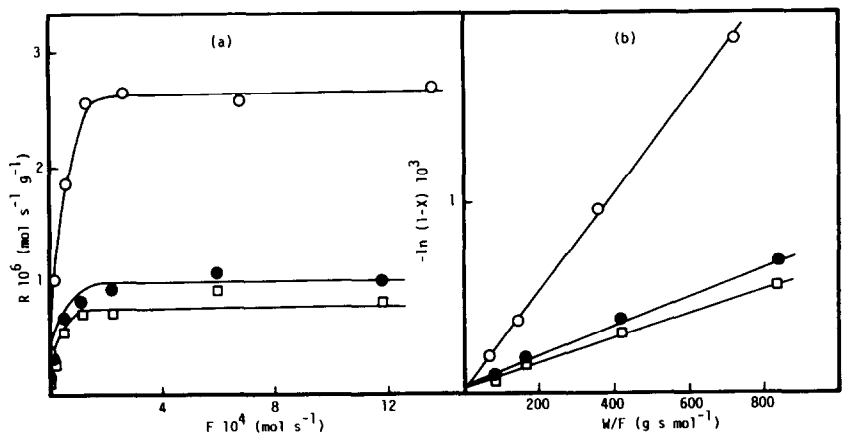

FIG. 1. (a) Dehydrogenation rate, R, of alkylbenzenes on 0.1 g of $Ni/AlPO_4$-F at 723 K as a function of feed rate, F. (b) Least-squares fit of Eq. (1) to the initial conversion data, X, at different residence time, W/F. (○) Ethylbenzene, (●) *n*-propylbenzene, (□) i-propylbenzene.

version was kept at a sufficient level (<0.5%) in order to be able to apply the "differential reactor" conditions for the treatment of the rate data.

A first-order rate equation was found to fit the data, Fig. 1b, at different residence times (lower than 800 g s mol^{-1})

$$\ln[1/(1 - X)] = k(W/F), \qquad (1)$$

where X is the conversion degree, defined as the number of moles of dehydrogenated alkylbenzene per mole of alkylbenzene fed. The slope of the straight lines yields the value of the reaction rate constant, k (in mol g^{-1} s^{-1}). These values are collected in Table 3 for the three alkylbenzenes with all the catalysts studied at 723 K.

The specific reaction rate constants values, k_s (in mol s^{-1} m_{Ni}^{-2}), are also shown. These k_s values, defined as the activity per unit surface area of supported or unsupported nickel metal, are obtained from k and the respective values of the metal surface area, S, in Table 2.

A significant fact to note is that the straight lines in Fig. 1b do not pass exactly through the origin when conversion is extrapolated to zero residence time. This fact could be indicative of some "residual" activity even in the absence of catalyst in the reactor. This is so because the reaction is able to take place in a negligible extension in the absence of the catalyst, especially at the highest temperatures. Furthermore, identical negligible activities are obtained when the different supports are used as catalysts. Accordingly it may be assumed in the present experimental conditions that the catalytic activity is exclusively developed on the nickel metal surface. Thus, the evolution of the catalytic activity with temperature has been studied taking this into account in order to apply the Arrhenius and Eyring equations to k_s values.

TABLE 3

Reaction Rate Constants, k (mol g^{-1} s^{-1}), and Specific Reaction Rates, k_s (mol s^{-1} m_{Ni}^{-2}), of Different Catalysts in the Dehydrogenation of the Alkylbenzenes Studied under Standard Conditions at 723 K

Catalyst	Ethylbenzene		*n*-Propylbenzene		i-Propylbenzene	
	10^6k	10^6k_s	10^6k	10^6k_s	10^6k	10^6k_s
$Ni/AlPO_4$-F	2.58	0.23	0.75	0.07	0.58	0.05
$Ni/AlPO_4$-P	1.14	0.18	1.14	0.18	0.92	0.14
Ni/SiO_2	3.02	0.34	0.82	0.09	1.77	0.20
Ni/Al_2O_3	0.47	0.09	0.19	0.03	0.12	0.02
Ni-bulk	0.31[a]	0.12	0.05[a]	0.02	0.06[a]	0.02

[a] In this case, the reactivity is due to 0.2 g of the catalyst that is the nickel loading in 1 g of the supported nickel systems.

Both equations evaluate the temperature dependence of reaction rates in terms of transition state theory by separating the enthalpy ($\Delta H^{\neq}$) and entropy ($\Delta S^{\neq}$) components which gives

$$k_s = (\kappa kT/h) \exp(\Delta S^{\neq}/R) \exp(-\Delta H^{\neq}/RT) = (\kappa kT/h) \exp(-\Delta G^{\neq}/RT) \qquad (2)$$

in which κ is the transmission coefficient, usually taken to be 1, k is Boltzmann's constant, h is Planck's constant, T is the absolute temperature, and $\Delta H^{\neq}$, $\Delta S^{\neq}$, and $\Delta G^{\neq}$ are respectively the enthalpy, entropy, and free-energy differences between reactants and the transition state.

The term $(\kappa kT/h) \exp(\Delta S^{\neq}/R)$ varies slightly with T compared to $\exp(-\Delta H^{\neq}/RT)$ because of the exponential nature of the latter. To a good approximation, then, we have the Arrhenius equation:

$$k_s = A \exp(-E_a/RT), \qquad (3)$$

where E_a is the apparent activation energy and A the Arrhenius preexponential factor.

The Eyring equation is directly obtained by taking the logarithm of Eq. (2):

$$\ln (k_s/T) = \ln (\kappa k/h) + \Delta S^{\neq}/R - \Delta H^{\neq}/RT. \qquad (4)$$

Thus, from the temperature dependence of the specific rate constant, k_s, we can derive $\Delta H^{\neq}$ (or E_a) and $\Delta S^{\neq}$ (or ln A).

In dealing with $\Delta S^{\neq}$ and $\Delta H^{\neq}$, it is necessary to point out that their values only relate the activated complex to the reac-

TABLE 4

Apparent Activation Energies, E_a (kJ mol^{-1}) and Arrhenius Constants, ln A (mol s^{-1} m$_{Ni}^{-2}$), with Their Respective Standard Deviations, for the Catalysts and Substrates Studied

Catalyst	Ethylbenzene		*n*-Propylbenzene		i-Propylbenzene	
	E_a	ln A	E_a	ln A	E_a	ln A
Ni/AlPO$_4$-F	49.14 ± 2.47	−7.14 ± 0.43	86.36 ± 2.05	−2.11 ± 0.33	118.55 ± 5.14	2.93 ± 0.79
Ni/AlPO$_4$-P	66.01 ± 3.97	−4.46 ± 0.61	71.37 ± 1.80	−3.62 ± 0.30	98.62 ± 3.51	0.69 ± 0.57
Ni/SiO$_2$	37.30 ± 2.09	−8.82 ± 0.37	80.50 ± 4.72	−2.77 ± 0.75	100.34 ± 3.55	1.31 ± 0.58
Ni/Al$_2$O$_3$	86.69 ± 3.89	−1.80 ± 0.60	129.81 ± 5.18	4.47 ± 0.83	161.50 ± 1.63	9.32 ± 0.25
Ni-bulk	34.37 ± 1.21	−10.25 ± 0.20	77.86 ± 0.42	−4.87 ± 0.12	84.18 ± 1.34	−3.56 ± 0.21

Note. Uncertainties are determined by standard deviations.

tants and are not relevant to the products. Thus, from $\Delta H^{\neq}$, we obtain the additional enthalpy content of the activated complex relative to the reactants. From $\Delta S^{\neq}$, a knowledge of the relative entropy of the activated complex compared to that of the reactant is obtained.

Table 4 shows the values of apparent activation energy, E_a, and the preexponential factor, ln A, and Table 5 the values of activation enthalpy, $\Delta H^{\neq}$, and activation entropy, $\Delta S^{\neq}$, obtained by plotting ln k_s vs T^{-1} (Fig. 2) and ln (k_s/T) vs T^{-1} (Fig. 3), respectively.

DISCUSSION

According to the results obtained, the nonoxidative dehydrogenation of EB, *n*-PB, and i-PB, in the present experimental conditions, may be explained within the framework of the Langmuir–Hinshelwood kinetic models, by the reversal of the steps of a classical Horiuti–Polanyi type noncompetitive mechanism (*33*), describing the hydrogenation of an olefinic double bond.

Thus, the negative values of $\Delta S^{\neq}$ indicate that, on going from the ground state to the transition state, an extensive restriction in the degrees of freedom must be considered. This highly ordered transition state is consistent with a reaction mechanism whose slowest step is the stabilization and immobilization of reactant molecules on catalyst active sites. With respect to this, the reaction rate is proportional to the quantity of adsorbed reactant molecules, and the reverse reaction is negligible. Besides, the relatively low $\Delta H^{\neq}$ values appear to be consistent with a concerted evolution in the limiting adsorption step which also must be associated with the low values of $\Delta S^{\neq}$. This fact is in accord with the results obtained

TABLE 5

Activation Enthalpies, $\Delta H^{\neq}$ (kJ mol^{-1}) and Activation Entropies $\Delta S^{\neq}$ (J mol^{-1} K^{-1}) with Their Respective Standard Deviations, for the Catalysts and Substrates Studied

Catalyst	Ethylbenzene		*n*-Propylbenzene		i-Propylbenzene	
	$\Delta H^{\neq}$	$\Delta S^{\neq}$	$\Delta H^{\neq}$	$\Delta S^{\neq}$	$\Delta H^{\neq}$	$\Delta S^{\neq}$
Ni/AlPO$_4$-F	43.45 ± 2.43	−320.23 ± 3.35	80.12 ± 2.13	−279.20 ± 2.93	112.02 ± 5.23	−237.76 ± 6.70
Ni-AlPO$_4$-P	59.36 ± 4.02	−299.30 ± 5.02	65.47 ± 1.80	−291.35 ± 2.51	92.47 ± 3.60	−255.76 ± 5.02
Ni/SiO$_2$	31.65 ± 2.05	−334.04 ± 2.93	73.00 ± 4.77	−286.32 ± 6.28	94.19 ± 3.51	−250.74 ± 4.60
Ni/Al$_2$O$_3$	82.05 ± 3.93	−277.11 ± 5.02	123.57 ± 5.27	−224.37 ± 7.12	155.05 ± 1.63	−184.60 ± 2.09
Ni-bulk	28.42 ± 1.26	−346.18 ± 1.67	71.62 ± 0.71	−301.39 ± 0.84	77.65 ± 1.34	−291.35 ± 1.67

Note. Uncertainties are determined by standard deviations.

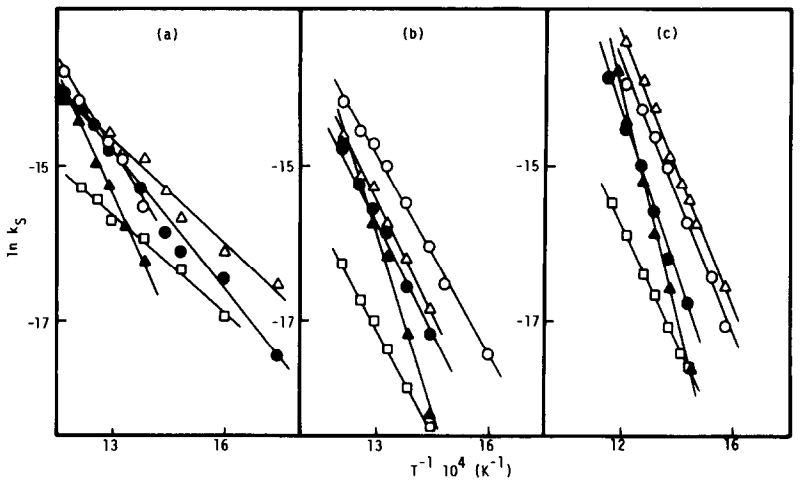

FIG. 2. Arrhenius plots for the dehydrogenation of (a) ethylbenzene, (b) *n*-propylbenzene, and (c) i-propylbenzene on nickel catalysts: (●) Ni/$AlPO_4$-F, (○) Ni-$AlPO_4$-P, (△) Ni/SiO_2, (▲) Ni/Al_2O_3, (□) Ni-bulk.

by Wang *et al.* (*27, 28*) in the nonoxidative dehydrogenation of ethylbenzene over TiO_2–ZrO_2 catalysts, which may be described through a concerted two-center mechanism, where zirconium ions act like Lewis acid, and titanium ions as a base.

However, the present work also establishes that acid and basic sites do not exhibit catalytic activity in the dehydrogenation of short-chain alkylbenzenes to alkenylbenzenes in nonoxidative conditions, contrary to that described for TiO_2–ZrO_2 catalysts (*27–30*), although in the present case we feel that the acid and base sites of each support plays an important part in determining the catalytic activity of the supported nickel through a metal–support interaction effect.

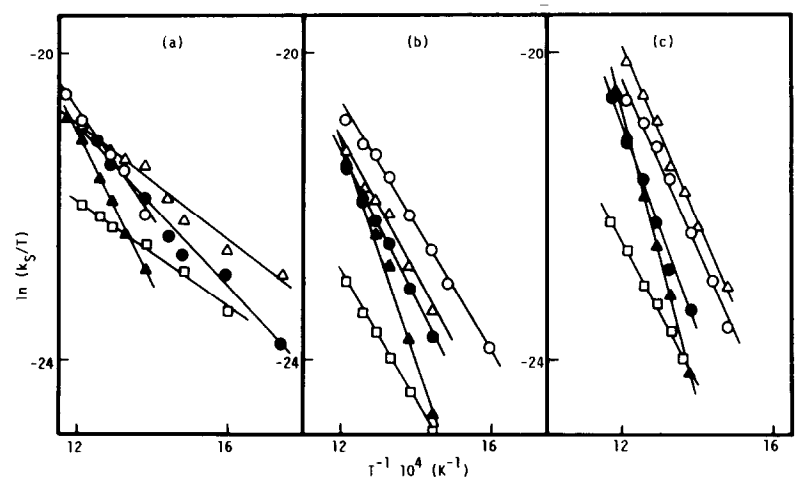

FIG. 3. Eyring plots for the dehydrogenation of (a) Ethylbenzene, (b) *n*-propylbenzene, and (c) i-propylbenzene on nickel catalysts: (●) Ni/$AlPO_4$-F, (○) Ni-$AlPO_4$-P, (△) Ni/SiO_2, (▲) Ni/Al_2O_3, (□) Ni-bulk.

Thus, from the results in Tables 1 and 2 we can see how the metal deposition, throughout the supports, induces a strong decrease in the number of acid sites, while the number of basic sites remain almost unchanged. This behavior is in very close agreement with those suggested by Bartholomew *et al.* (*34, 35*), which attributed the metal–support interaction to a transfer of electrons between the nickel atoms and the acid (oxidizing) sites on the support surface. According to Vannice and Garten (*36*), this preferential interaction through the oxidizing (or acid) sites of the support surface would reduce the *d*-band concentration of electrons in the metal crystallites shifting the metallic behavior of supported nickel to a catalytic behavior more characteristic of cobalt. With respect to this, we may understand that all the supports, with the sole exception of Al_2O_3, enhance the specific catalytic activity of nickel to a variable degree (k_s values in Table 3). Thus, the sequence obtained in the EB dehydrogenation

$$Ni/SiO_2 > Ni/AlPO_4\text{-}F \geq Ni/AlPO_4\text{-}P > Ni\text{- bulk} > Ni/Al_2O_3$$

is the same as that obtained with respect to the number of acid sites and opposite to the sequence regarding the number of basic sites in the nickel-supported catalysts (X_m values in Table 2.).

This double correlation is not so strictly obtained with the methyl derivatives of ethylbenzene, *n*-PB and i-PB, which exhibit, in the k_s values, the sequence

$$Ni/AlPO_4\text{-}P > Ni/SiO_2 > Ni/AlPO_4\text{-}F > Ni/Al_2O_3 \geq \text{Ni-bulk}.$$

However, in this case, also, there is close agreement between the acid–base properties of catalysts and their specific activity. Therefore, we have to conclude that it is impossible to extend the results obtained in the dehydrogenation of a substrate with a series of catalysts to other substrates because of the influence of substituent effects, not only in the electron density but also in the steric hindrance to adsorption in the reactant molecule.

These steric and electronic effects can be better evaluated from the values of activation energy, E_a, the frequency factor, ln A, in Table 4, and from the analogous quantities of activation enthalpy $\Delta H^{\neq}$ and activation entropy $\Delta S^{\neq}$, in Table 5, respectively. Thus, the variation in the magnitude of $\Delta H^{\neq}$ and $\Delta S^{\neq}$ with different substrates or due to the influence of different supports reflects their influence on the transition state structure. Since the $\Delta H^{\neq}$ value reflects the difference between the internal energy of the activated complex and the reactants, it will also be related to the electronic state of the substrate and catalyst, while the $\Delta S^{\neq}$ value (which is a measure of the degree of order or disorder produced in the formation of the activated complex) ought to be related first of all to the steric effects of reactants and/or the catalyst.

In agreement with these general ideas we see that an increase in $\Delta H^{\neq}$ and $\Delta S^{\neq}$ in the order i-PB > *n*-PB > EB in all catalysts indicates, according to Eq. (2), that the electronic effects of the methyl group associated to the enthalpy factor diminish the reactivity while the steric effects of the methyl group promote an increase in the translational, vibrational, or rotational degrees of freedom in the activated complex, as indicated by the increase in $\Delta S^{\neq}$ values, leading to an enhancement in the reactivity. Thus, the methyl substitution in the EB molecule clearly influences the catalytic dehydrogenation rate both through its electronic nature and by a steric effect on the conformational equilibrium in adsorption.

Similarly, support effects may be interpreted in this context. As may be seen, as a consequence of the metal–support interaction, $\Delta H^{\neq}$ and $\Delta S^{\neq}$ values are decreased in the order

$$Ni/Al_2O_3 > Ni/AlPO_4\text{-}P > Ni/AlPO_4\text{-}F > Ni/SiO_2 > \text{Ni-bulk}$$

in EB dehydrogenation while the corresponding values in its two methylderivatives i-PB and *n*-PB follows the similar sequence

$$Ni/Al_2O_3 > Ni/AlPO_4\text{-}F > Ni/SiO_2 > Ni/AlPO_4\text{-}P > Ni\text{-bulk}.$$

Accordingly, the restriction of molecular freedom and the additional enthalpy content of the activated complex relative to the reactants are decreased, in these same orders. In fact, according to Eq. (2), the metal–support interaction effects enhance the catalytic activity through the contribution of the steric effects, given by $\Delta S^{\neq}$, unlike the contribution of inductive effects, given by $\Delta H^{\neq}$, which decrease the reactivity.

In summary, the role played by the support on the reactivity of Ni-supported catalysts is similar to that of the methyl substitution on EB because in both cases, on increasing $\Delta H^{\neq}$ and $\Delta S^{\neq}$ values, the same two opposite effects on the catalytic activity develop. There is a trend to increase it caused by the increase in $\Delta S^{\neq}$, together with a decrease caused by the increase in $\Delta H^{\neq}$ values. This behavior offers some interesting fundamental problems which need to be clarified. Thus, in spite of the fact that $\Delta H^{\neq}$ values are appreciably greater than $\Delta S^{\neq}$ values (Table 5) we have to consider that according to Eq. (2) the contribution of the entropy factor given by $\Delta S^{\neq}/R$ is, in the present experimental conditions, higher than those relative to the enthalpy factor $(-\Delta H^{\neq}/RT)$, which is strongly determined by the temperature, as shown in Table 6 where their corresponding values at 723 K are collected.

On the basis of these results we can understand that the metal–support interaction effects enhance the catalytic activity by enhancing the entropy factor which is the term that contributes in the greatest proportion to k_s values in the present experimental conditions.

However, the negative influence of the enthalpy factor increases at the same time; the former effect predominates resulting in the stabilization of the reaction complex and a faster reaction. Besides, it is now becoming evident that on increasing the reaction temperature, the positive influence of the nickel–support interaction effects on k_s would be increased as the reaction temperature increases. This occurs because, while entropy contribution is constant, the influence of enthalpy is inversely proportional to the reaction temperature; consequently, its negative influence is strongly decreased.

On the other hand, there is a relationship between the values of $\ln A$ and E_a, in Table 4, as shown in Fig. 4, known as the "compensation effect" or the "isokinetic relationship" (IKR) (*37–39*) that can be expressed (*40*) by

$$\ln A = \ln \alpha + E_a/\theta R, \qquad (5)$$

TABLE 6

Contribution to the Specific Catalytic Activity, k_s, from the Entropy Factor, $\Delta S^{\neq}/R$, and from the Enthalpy Factor, $-\Delta H^{\neq}/RT$, at 723 K in the Dehydrogenation of EB, *n*-PB, and i-PB in Every Catalyst Studied

Catalyst	Ethylbenzene		*n*-Propylbenzene		i-Propylbenzene	
	$-\Delta H^{\neq}/RT$	$\Delta S^{\neq}/R$	$-\Delta H^{\neq}/RT$	$\Delta S^{\neq}/R$	$-\Delta H^{\neq}/RT$	$\Delta S^{\neq}/R$
$Ni/AlPO_4$-F	−7.23	−38.53	−13.33	−33.60	−18.64	−28.61
$Ni/AlPO_4$-P	−9.88	−36.02	−10.90	−35.06	−15.39	−30.77
Ni/SiO_2	−5.27	−40.20	−12.15	−34.45	−15.68	−30.17
Ni/Al_2O_3	−13.66	−33.35	−20.57	−27.00	−25.81	−22.21
Ni-bulk	−4.76	−41.66	−11.92	−36.27	−12.92	−35.06

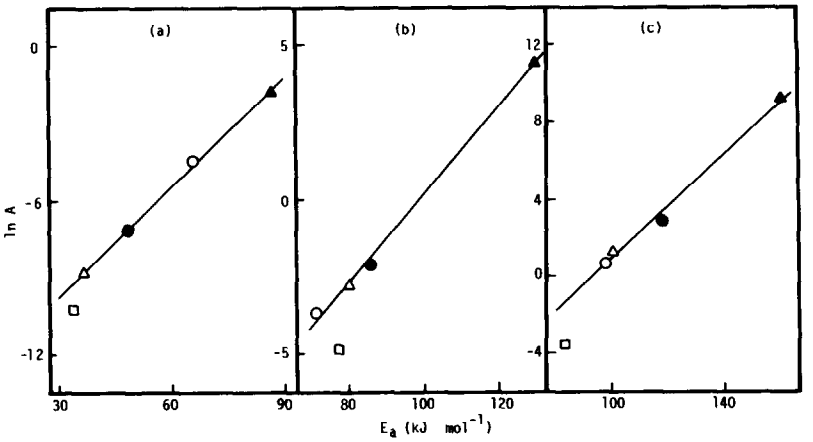

FIG. 4. Compensation effect between E_a and ln A for (a) ethylbenzene, (b) *n*-propylbenzene, and (c) i-propylbenzene with all catalysts: (●) Ni/$AlPO_4$-F, (○) Ni-$AlPO_4$-P, (△) Ni/SiO_2, (▲) Ni/Al_2O_3, (□) Ni-bulk.

where R is the gas constant and θ is the "isokinetic temperature" at which identical values of specific reaction rate constant, $k_s = \alpha$. are obtained. According to the Arrhenius expression when A is expressed by Eq. (5) we have

$$k_s = \alpha \exp[(E_a/R)(1/\theta - 1/T)]. \quad (6)$$

Thus, below θ, the reactions with lower E_a exhibit higher reaction rates and, above θ the inverse is true.

In fact the plots of ln A vs E_a in Fig. 4, for each substrate, are linear for all catalysts with regression coefficients over 0.99 when unsupported nickel is not considered. Therefore, from the slopes and intercepts, the α and θ parameters (α_s and θ_s) for all three alkylbenzenes studied are obtained. They are collected in Table 7.

Furthermore, the plots of ln A vs E_a in Table 4 for each catalyst, with the three alkylbenzenes are also linear with high regression coefficients (above 0.99). Accordingly, from slopes and intercepts we now obtain the α and θ values for different catalysts (α_c and θ_c) shown in Table 8. Thus, it is possible to obtain two parameters, α_s and θ_s, closely associated to the substrates and, at the same time, α_c and θ_c values exclusively related to the catalysts.

Although the most habitual representation of compensation effect is through Eq. (5), it also may be obtained from an entropy–enthalpy relationship because,

TABLE 7

Values of α_s and $\theta_s{}^a$ Obtained from the Representation of ln A vs E_a and Values of $\theta_s{}^b$, $\Delta G^{\neq}_s$ and ln $K^{\neq}_s$, Obtained from the Representation of $\Delta H^{\neq}$ vs ΔS^c

Substrate	α_s 10^6 (mol/s m^2_{Ni})	$\theta_s{}^a$ (K)	$\theta_s{}^b$ (K)	$\Delta G^{\neq}_s$ (KJ/mol)	ln $K^{\neq}_s$
Ethylbenzene	0.737 ± 0.015	838.70 ± 28.80	843.63 ± 26.72	313.22 ± 8.23	−44.66 ± 1.17
n-Propylbenzene	0.714 ± 0.059	841.95 ± 43.89	839.45 ± 43.81	312.48 ± 11.90	−44.77 ± 2.89
i-Propylbenzene	3.562 ± 0.296	893.76 ± 56.59	888.60 ± 57.00	319.78 ± 15.97	−43.28 ± 3.52

Note. Uncertainties are determined by their respective standard deviations.

TABLE 8

Values of α_c and θ_c[a] Obtained from the Representation of ln A vs E_a and Values of θ_c[b], $\Delta G^{\neq}_{\bar{c}}$ and ln $K^{\neq}_{\bar{c}}$, Obtained from the Representation of $\Delta H^{\neq}$ vs $\Delta S^{\neq}$

Catalyst	α_c 10^6 (mol/s m^2_{Ni})	θ_c[a] (K)	θ_c[b] (K)	$\Delta G^{\neq}_{\bar{c}}$ (kJ/mol)	ln $K^{\neq}_{\bar{c}}$
Ni/$AlPO_4$-F	0.578 ± 0.022	830.54 ± 35.71	831.62 ± 35.76	310.61 ± 10.05	−44.92 ± 2.42
Ni/$AlPO_4$-P	0.340 ± 0.001	760.73 ± 32.70	760.32 ± 1.23	286.94 ± 0.35	−45.39 ± 0.09
Ni/SiO_2	0.341 ± 0.028	762.51 ± 76.84	756.78 ± 75.85	286.03 ± 22.18	−45.46 ± 5.76
Ni/Al_2O_3	0.410 ± 0.007	809.86 ± 11.07	809.99 ± 10.21	304.89 ± 2.37	−45.27 ± 0.45
Ni-bulk	0.387 ± 0.016	922.16 ± 63.78	918.15 ± 55.43	346.59 ± 17.40	−45.40 ± 3.56

Note. Uncertainties are determined by their respective standard deviations.

according to Boudart (*41*), the general explanation of this fact is the existence of a LFER which manifests itself in a linear relation between enthalpy and entropy in the activated complex for any set of reactions of the same type exhibiting the same value of activation free energy, $\Delta G^{\neq}$, over the experimental temperature range. This constant on $\Delta G^{\neq}$ lets us determine not only θ but also this $\Delta G^{\neq}$ constant value and the equilibrium constant of the activated complex, $K^{\neq}$, which is also a constant according to the general expression

$$\Delta G^{\neq}_{\text{const.}} = -\theta R \ln K^{\neq} = \Delta H^{\neq} - \theta \Delta S^{\neq}. \quad (7)$$

Thus, from slopes and intercepts of the plots $\Delta H^{\neq}$ against $\Delta S^{\neq}$ we obtain the values of θ, $\Delta G^{\neq}$, and $K^{\neq}$ for each substrate (θ_s, $\Delta G^{\neq}_s$ and $K^{\neq}_s$) and all the catalysts (θ_c, $\Delta G^{\neq}_{\bar{c}}$, and $K^{\neq}_{\bar{c}}$) which are also quoted in Tables 7 and 8, respectively.

Furthermore, a simple method has recently become available (*42–45*) for testing whether or not the compensation effect obtained can be ascribed to a false correlation caused by a scatter of data due to the compensation of errors on both parameters $\Delta H^{\neq}$ and $\Delta S^{\neq}$, respectively. This method is based on the existence of a common point of intersection in the set of straight lines obtained in the Arrhenius or Eyring representation (Fig. 2 and 3). So far Linert *et al.* (*43–45*) have determined the intersection point in a set of equations where the rate constants were derived from the statistical theory of kinetics using the Exner analysis (*46, 47*) but it is evident that this method can be employed directly with Arrhenius or Eyring equations because according to them (*43*) "the correct procedure to demonstrate the IKR is to go back one step closer to the experiment and to examine if there is a common point of intersection in the Arrhenius plot (activation plot)." Besides, when we do it not only is it possible to determine the correctness of the IKR by applying the F-test or that proposed by Linert *et al.* (*42*), but also to obtain the θ, α, $\Delta G^{\neq}_{\text{const.}}$ or $K^{\neq}$ parameters. Thus, from the Arrhenius equation, α and θ are obtained from the abscis ($x = 1/\theta$) and ordinate ($y = \ln \alpha$) of the intersection point while from the Eyring equation $x = 1/\theta$ and $y = \ln [(\kappa k/h)K^{\neq}]$, and $\Delta G^{\neq}_{\text{const.}}$ is obtained from $K^{\neq}$ values (Eq. (7)).

These common points of intersection were obtained by applying a computer program similar to that described by Linert (*42*) to the experimental data in Fig. 2 and 3 (ln k_s vs $1/T$ and ln k_s/T vs $1/T$, respectively), and the values of θ, $\Delta G^{\neq}$, α, and $K^{\neq}$ parameters for substrates and catalysts thus obtained were practically coincidental, within experimental error, to those collected in Tables 7 and 8. Moreover, when Ni unsupported is considered in the determination of substrate parameters, there is also an important standard deviation that is

strongly diminished when excluded. Accordingly, the isokinetic hypothesis in the heterogenous gas-phase dehydrogenation reactions must be accepted, independently of the absence of a definitive theoretical explanation for this phenomenon. The empirical parameters obtained can give us valuable information not only on the substituent effects, such as the general application of the LFER described in homogeneous processes, but also on the catalyst effects.

Thus, according to the classification of Blackadder and Hinshelwood (*48*) the catalytic (nonoxidative) dehydrogenation on alkylbenzenes in the present experimental conditions ought to be considered enthalpy controlled ($\theta > T_{exp}$). Indeed, we have always operated below θ where the reactions with lower E_a exhibit higher reaction rates so the sequence obtained in the substrate reactivity (EB > *n*-PB ≥ i-PB) is the opposite of that in the E_a and θ_s values (Tables 4 and 7). This fact is in accord with what might be expected from Eq. (6), where the activity k_s is proportional to exp $(1/\theta)$, and according to this exponential nature of both parameters (E_a and θ), their contributions on k_s are much more important than those of α values. Besides, according to Eq. (2), $\Delta G_s^{\neq}$ values (in Table 7) are inversely related to reactivity, k_s, and they are better parameters than $K_s^{\neq}$ to determine structure–reactivity correlations. This is because the former parameter ($\Delta G_s^{\neq}$) can be regarded as insensitive to temperature while $K_s^{\neq}$ represents the value of the equilibrium constant of the activated complex at θ_s temperature (Eq. (7)); likewise, α_s represents the reactivity at this θ_s temperature.

Similarly, the values of θ_c and $\Delta G_c^{\neq}$ may account for the sequences obtained for k_s values in the dehydrogenation of each substrate (EB, *n*-PB, or i-PB) with different catalysts. Thus, the enhancement of the specific catalytic activity of nickel catalysts due to the effects of metal–support interaction can be associated with the lessening of θ_c and $\Delta G_c^{\neq}$ values which, in this sense, may be taken as a measure of the extent of this interaction.

Finally, we may understand the high deviation of Ni-bulk in determining the IKR for substrates by taking into account the relatively important difference between $\Delta G_c^{\neq}$ for Ni-bulk and all those of the remaining Ni-supported catalysts exhibiting very close values. That is, the compensation effect is obtained as a consequence of the proximity of the respective $\Delta G^{\neq}$ values.

CONCLUSIONS

From this study we can conclude that, like that obtained in the liquid-phase hydrogenation of the olefinic double bond (*1*), the gas-phase dehydrogenation of alkylbenzenes, over the same supported nickel catalysts, exhibits an IKR or "compensation effect" which manifests itself through a linear relationship between the activation parameters $\Delta H^{\neq}$ and $\Delta S^{\neq}$, due to the existence of a LFER. As a consequence of this fact, it is possible to obtain a series of isokinetic parameters, θ, $\Delta G^{\neq}$, $K^{\neq}$, and α, that may provide a more general measurement of the reactivity characteristic of a series of related reactions and/or catalysts in the gas or liquid phase. Valuable information is also obtained on the reaction mechanism because, if an IKR holds for a reaction series, a single common interaction mechanism can be expected (*40, 42, 49*).

In agreement with these general ideas, the existence of LFER manifesting itself through isokinetic relationships in series of related reactions seems to be almost universal characteristic of heterogeneous catalysis with the need of only one requirement; that is, the reaction rates ought to be controlled by a chemical step. Thus, it is necessary to determine the rate of operating variables where the kinetic data are free from transport influences. This, in general, is much easier to obtain in the liquid than in the gas phase so it has long been thought

that the compensation effect is a specific feature of liquid-phase reactions (*2*). However, when in the gas phase, the experiments are developed in the kinetic region, as in the present work, isokinetic relationships arise which permit us to obtain a series of isokinetic parameters that are able to explain the sequences obtained in the catalytic activity of substrates and catalysts or even to constitute a measure of the metal–support interaction.

Consequently the method of LFER that is still the most practical for predicting substituent effects for homogeneous reactions in liquid solutions (*3*), when applied to the catalytic heterogeneous process through IKR, may constitute a promising technique for measuring the existence and extent of metal–support interactions. That is, it supplies data specifically concerning the catalytically active part of the metal surface. In connection with this, the important role played by the acid–basic nature of the support in determining the extent of the metal–support interaction is also established.

ACKNOWLEDGMENTS

The financial support of the Consejería de Educación de la Junta de Andalucía (1985) is gratefully acknowledged. Also the authors acknowledge the grammatical revision of the manuscript carried out by M. Sullivan and the valuable help of Dr. J. M. Rodriguez of the Departamento de Química Física de la Universidad de Córdoba, in the computer and statistical analysis of the data.

REFERENCES

1. Campelo, J. M., Garcia, A., Luna, D., and Marinas, J. M., *J. Catal.* **97,** 108 (1986).
2. Schmid, R., and Sapunov, V. N., "Non-formal Kinetics," Chap. 10. Verlag Chemie, Weinheim, 1982.
3. Grunwald, E., and Leffler, J. E., "Physical Chemistry: An Advanced Treatise" (H. Eyring, Ed.), Vol. 7, Chap. 4, p. 212. Academic Press, New York, 1975.
4. Kraus, M., *Adv. Catal. Relat. Subj.* **17,** 75 (1967), and references cited therein.
5. K. Kearby, *in* "Proceedings, 2nd International Congress on Catalysis, Paris, 1960," p. 2567. Technip, Paris, 1961.
6. Campelo, J. M., Garcia, A., Luna, D., and Marinas, J. M., *Appl. Catal.* **3,** 315 (1982).
7. Campelo, J. M., Garcia, A., Luna, D., and Marinas, J. M., *Bull. Soc. Chim. Belg.* **91,** 131 (1982).
8. Campelo, J. M., Garcia, A., Luna, D., and Marinas, J. M., *Bull. Soc. Chim. Belg.* **92,** 851 (1983).
9. Campelo, J. M., Garcia, A., Gutierrez, J. M., Luna, D., and Marinas, J. M., *Appl. Catal.* **7,** 307 (1983).
10. Marcelin, G., and Vogel, R. F., *J. Catal.* **82,** 482 (1983).
11. Marcelin, G., Vogel, R. F., and Swift, H. E., *J. Catal.* **83,** 42 (1983).
12. Marcelin, G., Vogel, R. F., and Swift, H. E., *Ind. Eng. Chem. Prod. Res. Dev.* **23,** 41 (1984).
13. Campelo, J. M., Garcia, A., Luna, D., and Marinas, J. M., *J. Chem. Soc., Faraday Trans. 1* **80,** 659 (1984).
14. Marcelin, G., and Lester, J. E., *J. Catal.* **93,** 270 (1985).
15. Marcelin, G., Vogel, R. F., and Swift, H. E., *J. Catal.* **98,** 64 (1986).
16. Beck, W. R., *J. Amer. Ceram. Soc.* **32,** 147 (1949).
17. Mooney, R. C. L., *Acta Crystallogr.* **9,** 728 (1956).
18. Peri, J. B., *Discuss. Faraday Soc.* **52,** 55 (1951).
19. Marinas, J. M., Jimenez, C., Campelo, J. M., Aramendia, M. A., Borau, V., and Luna, D., "7th Iberoamerican Symposium on Catalysis, La Plata," p. 79 (1980).
20. Moffat, J. B., *Catal. Rev. Sci. Engn.* **18,** 199 (1978).
21. Haber, J., and Szybaltska, V., *Discuss. Faraday Soc.* **72,** 263 (1981).
22. Itoh, H., Tada, A., and Hattori, H., *J. Catal.* **76,** 235 (1982).
23. Campelo, J. M., Garcia, A., Gutierrez, J. M., Luna, D., and Marinas, J. M., *Canad. J. Chem.* **61,** 2567 (1983).
24. Campelo, J. M., Garcia, A., Luna, D., and Marinas, J. M., *Canad. J. Chem.* **62,** 638 (1984).
25. Cabello, J. A., Campelo, J. M., Garcia, A., Luna, D., and Marinas, J. M., *J. Org. Chem.* **49,** 5195 (1984).
26. Campelo, J. M., Garcia, A., Gutierrez, J. M., Luna, D., and Marinas, J. M., *Colloids Surf.* **8,** 353 (1984).
27. Wang, I., Chang, W. F., Shian, R. J., Wu, J. C., and Chung, C. S., *J. Catal.* **83,** 428 (1983).
28. Wu, J. C., Chung, C. S., Ay, C. L., and Wang, I., *J. Catal.* **87,** 98 (1984).
29. Wang, I., Wu, J. C., and Chung, C. S., *Appl. Catal.* **16,** 89 (1985).
30. Wu, J. C., Chung, C. S., and Wang, I., *Appl. Catal.* **18,** 295 (1985).
31. Moss, R. L., "Experimental Methods in Catalytic Research" (R. B. Anderson and P. T. Dawson, Eds.), Vol. 2, Chap. 2, p. 43. Academic Press, New York, 1976.

32. Campelo, J. M., Garcia, A., Luna, D., and Marinas, J. M., *Colloids Surf.* **5,** 227 (1982).
33. Ledoux, M., and Gault, F. G., *J. Catal.* **60,** 15 (1979).
34. Bartholomew, C. H., and Pannell, R. B., *J. Catal.* **65,** 390 (1980).
35. Bartholomew, C. H., Panell, R. B., and Butler, J. L., *J. Catal.* **65,** 335 (1980).
36. Vannice, M. A., and Garten, R. L., *J. Catal.* **63,** 255 (1980).
37. Cremer, E., *Adv. Catal.* **7,** 75 (1955).
38. Galwey, A., *Catal. Rev.* **26,** 247 (1977).
39. Shakparanov, M. I., and Evdokimov, K. Yu., *Russ. J. Phys. Chem.* **56,** 1270 (1982).
40. Conner, W. C., Jr., *J. Catal.* **78,** 238 (1982).
41. Boudart, M., "Kinetics of Chemical Processes," p. 167. Prentice-Hall, Englewood Cliffs, NJ, 1968.
42. Linert, W., Soukup, R. W., and Schmid, R., *Compt. Chem.* **6,** 47 (1982).
43. Linert, W., Kudrjawtsev, A. B., and Schmid, R., *Aust. J. Chem.* **36,** 1903 (1983).
44. Linert, W., and Kudrjawtsev, A. B., *Aust. J. Chem.* **37,** 1139 (1984).
45. Linert, W., Schmid, R., and Kudrjawtsev, A. B., *Aust. J. Chem.* **38,** 677 (1985).
46. Exner, O., *Prog. Phys. Org. Chem.* **10,** 411 (1973).
47. Exner, O., and Beraneck, V., *Collect. Czech. Chem. Commun.* **38,** 781 (1973).
48. Blackadder, D. A., and Hinshelwood, C., *J. Chem. Soc.,* 2727 (1958).
49. Galwey, A., and Brown, M., *J. Catal.* **60,** 335 (1979).